

Rapid annealing of silicon with a scanning cw Hg lamp

T. J. Stultz,^{a)} J. Sturm, and J. F. Gibbons
Stanford Electronics Laboratory, Stanford, California 94305

S. K. Ichiki
Lockheed Palo Alto Research Laboratory, Palo Alto, California 94304

(Received 17 May 1982; accepted for publication 2 July 1982)

A scanning arc lamp annealing system has been built using a 3-in.-long mercury arc lamp with an elliptical reflector. The reflector focuses the light into a high intensity narrow line source. Silicon wafers implanted with 100-KeV $^{75}\text{As}^+$ to $1 \times 10^{15} \text{ cm}^{-2}$ have been uniformly annealed with a single scan, resulting in complete activation and negligible redistribution of the implanted species. Using a scan rate of 1 cm/s, entire 3-in. wafers have been annealed in less than 10 sec with this system.

PACS numbers: 81.40.Ef

Over the past few years, a considerable amount of research has been directed towards developing alternative heat treatment techniques for application to semiconductor processing. The most thoroughly investigated of these has been the use of pulsed and cw laser and electron beams.¹ Work performed using these sources has provided new insights into the mechanisms of thermally induced processes, such as solid-phase and liquid-phase epitaxial growth and thin-film recrystallization. In particular, some of the earliest work demonstrated that ion implantation damaged silicon could be annealed with a scanned cw laser such that there was complete electrical activation of the implanted species and virtually no impurity redistribution.² This was accomplished by raising the temperature of the material sufficiently to fully anneal out the damage ($\sim 1000^\circ\text{C}$), but for short enough times to prevent significant diffusion of the implanted species.

Once this process was understood, work began to identify alternative annealing techniques which offered the same advantage of diffusionless annealing. Most recently, incoherent light sources have been shown to be very effective for rapidly annealing ion implanted silicon.³⁻⁸ This approach has several distinct advantages over other techniques, in particular laser annealing. First, because the light is incoherent, interference effects which result from the interaction of monochromatic light and the dielectric layers on the semiconductor material are eliminated. These effects can lead to nonuniform heating of the irradiated material, if not eliminated. Second, the effective processing area for an arc lamp is orders of magnitude greater than that for a laser. For example, an entire silicon wafer can be annealed in about 10 sec, whereas a cw laser takes several tens of minutes to process the same amount of material. Finally, an arc lamp is significantly less expensive than a laser and is much more efficient to operate.

We have built an arc lamp annealing system which consists of a 3-in.-long high-pressure mercury lamp, an elliptically shaped reflector, and a variable speed translation hot stage. In previous work, xenon and krypton lamps were used. We chose to use a mercury lamp primarily for the following two reasons. The spectral distribution of this lamp is most heavily weighted in the uv range. Consequently, the

mean absorption depth for this source is much shallower than that for the other lamps. Specifically, the fraction of light absorbed versus depth is given by

$$F = I(\lambda)[1 - R(\lambda)]\{1 - \exp[-\alpha(\lambda)x]\}, \quad (1)$$

where $I(\lambda)$ is the wavelength dependent radiation intensity, $R(\lambda)$ is the wavelength dependent reflectivity, and $\alpha(\lambda)$ is the wavelength dependent absorption coefficient. Using published absorption and reflectivity data for silicon and the spectral distributions for xenon, krypton, and mercury lamps, the percent of incident light absorbed versus depth in silicon was calculated for each of the lamps. These data are given in Fig. 1. In thin-film processes, such as annealing and recrystallization, the region of interest is generally less than $1 \mu\text{m}$ thick. As shown in Fig. 1, the fraction of light absorbed from a mercury lamp in this region is more than twice that for the other lamps.

It should be noted that the absorption analysis presented is based on room temperature absorption data. Since the absorption coefficient of silicon increases with increasing temperature, the differences indicated will diminish as the temperature of the irradiated material increases. This change will not, however, change the relative weighting of the absorptive characteristic of the sources used.

The second reason the mercury lamp was chosen over

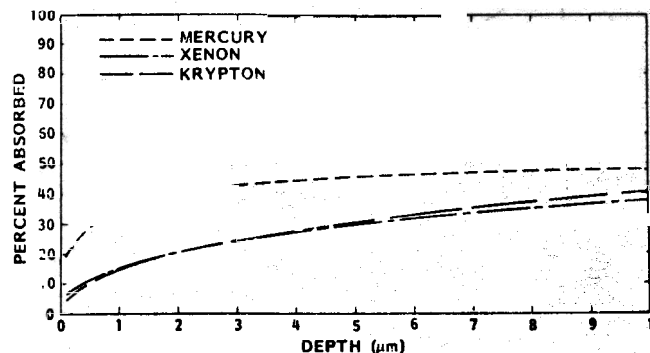


FIG. 1. Percent of incident light absorbed vs depth into silicon for three different sources.

^{a)} Also, Lockheed Palo Alto Research Laboratory.

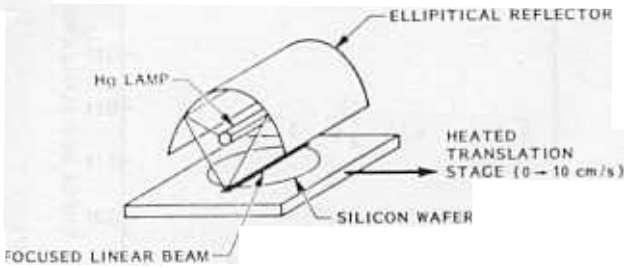


FIG. 2. Schematic representation of scanning cw arc lamp annealing system.

the other available lamps is due to the narrow capillary used for containing the discharge. For example, a typical 3-in. krypton lamp has a 5-mm capillary, whereas the mercury lamp uses a 2-mm capillary. The tighter confinement results in a narrower imaged beam, and thus yields a higher intensity at the sample surface for a given lamp power.

The light from the lamp is focused into a narrow (< 5 mm wide) ribbon by a 4-in.-long reflector with an elliptical cross section. By using this shape of reflector to collect and focus the light, we can create an intense linear heat source, and still maintain a reasonable working distance between the sample and the lamp. The reflector in our system has major and minor axes of 10 and 8.6 cm, respectively. This configuration gives a magnification factor of about 3.2, and a working distance of about 26 mm between the edge of the reflector and the focal plane.

Finally, the samples are placed on a heated sample stage, which can be translated beneath the lamp at speeds up to 10 cm/s. A schematic representation of the arc lamp annealing system is shown in Fig. 2.

Annealing experiments were carried out using 2- and 3-in. 1-8 Ω cm p -type (100) silicon wafers, which were implanted with $^{75}\text{As}^+$ at 100 keV to $1 \times 10^{15} \text{ cm}^{-2}$. It was found that several combinations of arc lamp power, scan

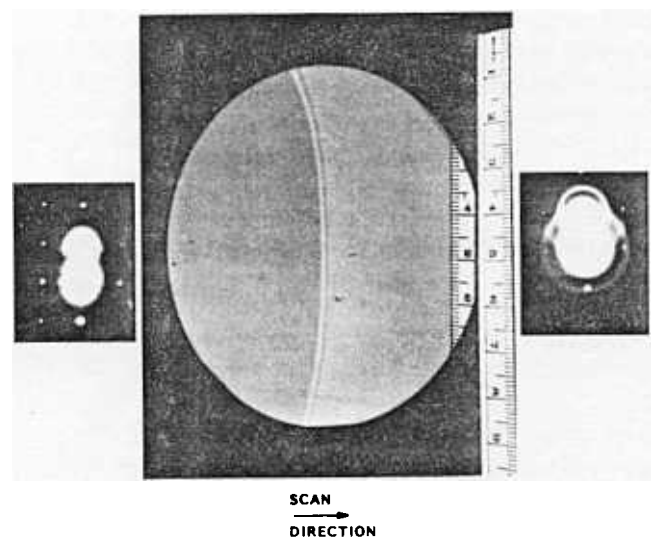


FIG. 3. Photograph of a partially annealed silicon wafer, and TEM diffraction patterns from the annealed and unannealed regions.

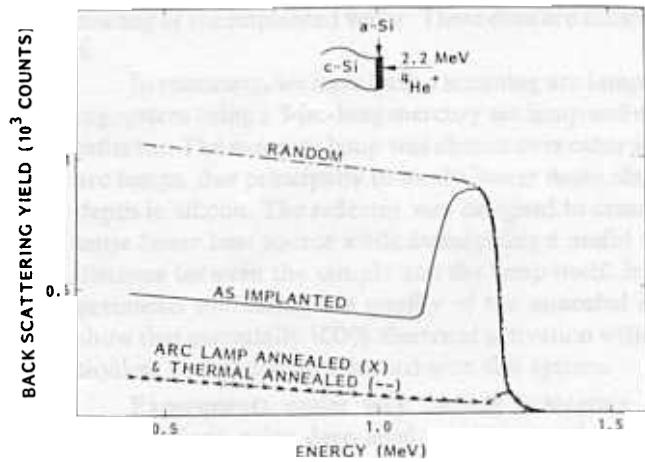


FIG. 4. Rutherford backscattering spectra from as-implanted, arc lamp annealed, and thermally annealed samples.

rate, and substrate temperature could be used to achieve a wafer temperature sufficient for good annealing, $\sim 1000^\circ\text{C}$. In general, scan rates from 5 mm/s to 1 cms, substrate temperatures of 400 to 600 $^\circ\text{C}$, and arc lamp input power of 1 to 1.5 kW/in. gave good results.

Because of the length of the arc lamp, an entire wafer can be annealed in a single scan. Figure 3 is a photograph of a 3-in. wafer in which the scan was stopped at the center of the wafer. Because of the difference in reflectivities between single crystal and amorphous silicon, the demarcation between the annealed and unannealed regions is readily seen. Transmission electron microscope (TEM) diffraction patterns made from samples taken from the unannealed and annealed regions clearly indicate the amorphous and completely re-

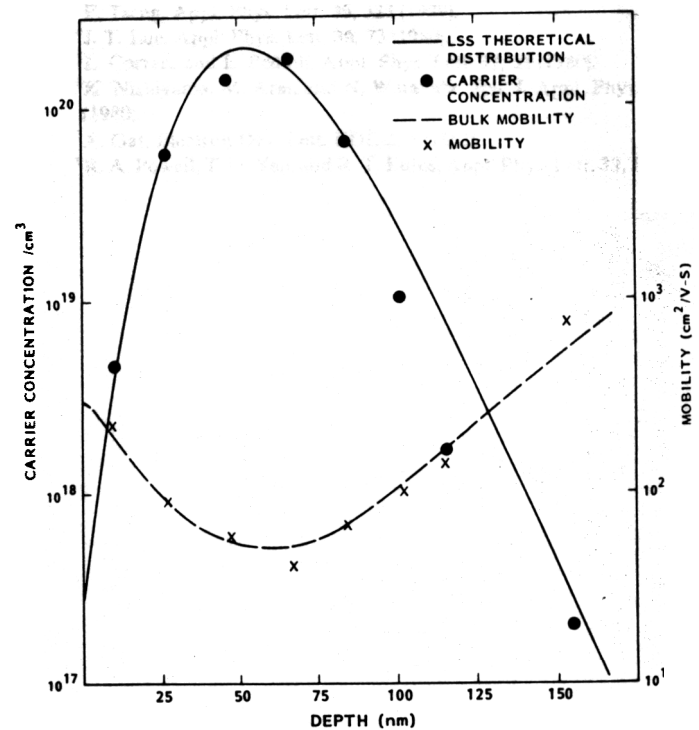


FIG. 5. Carrier concentration and mobility vs depth from an arc lamp annealed sample.

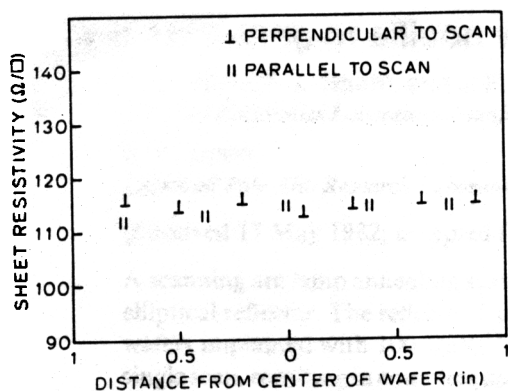


FIG. 6. Sheet resistivity profiles across an arc lamp annealed wafer.

crystallized nature of the regions, respectively. (The picture is somewhat distorted due to the angle at which the photo was taken.)

The recrystallized layer was also analyzed by Rutherford Backscattering Spectroscopy (RBS) and directly compared to a sample, which was thermally annealed at 850 °C for 30 min, followed by a 10-sec 1000 °C anneal. Figure 4 shows the backscattering spectra from an as-implanted, arc lamp annealed and thermally annealed sample. As shown, there is no detectable difference between the quality of the regrown material annealed by the scanned arc lamp and the thermally processed sample.

Carrier concentration and mobility of the scanning arc lamp annealed material as a function of depth were determined by means of differential sheet resistivity and Hall effect together with an anodic oxidation stripping technique. These results are shown in Fig. 5, along with the as-implanted profile calculated using LSS theory and published bulk silicon mobilities for the respective impurity concentrations. As shown, no measurable dopant redistribution occurred during the annealing process, and the free-carrier mobility in the annealed region is as good as found in bulk silicon.

Finally, to assess the uniformity of the anneal, four-point probe sheet resistivity measurements were made on a wafer, which was completely annealed in a single scan. The variation across the wafer from side to side and top to bottom

(with respect to the scanning beam) showed no significant variation in either direction, indicating a very uniform annealing of the implanted wafer. These data are shown in Fig. 6.

In summary, we have built a scanning arc lamp annealing system using a 3-in.-long mercury arc lamp and elliptical reflector. The mercury lamp was chosen over other available arc lamps, due principally to its shallower mean absorption depth in silicon. The reflector was designed to create an intense linear heat source while maintaining a useful working distance between the sample and the lamp itself. Initial experiments evaluating the quality of the annealed material show that essentially 100% electrical activation with a diffusionless anneal can be achieved with this system.

Experiments under way include evaluating the annealed silicon using deep-level transient spectroscopy, and extending the use of the scanning arc to other materials systems (e.g., GaAs, HgCdTe) and processes (e.g., thin-film recrystallization).

The authors wish to thank R. Pacquett and D. Torgerson for their helpful discussions, and D. Reynolds for his continued interest and support of this work. This work has been supported by Lockheed Missiles and Space Co., Inc. and DARPA Contract No. MDA 903-81-C-0294.

¹See, for example, *Laser and Electron Beam Solid Interactions and Materials Processing*, edited by Gibbons, Hess, and Sigmon (North-Holland, New York, 1981).

²A. Gat, J. F. Gibbons, T. J. Magee, J. Peng, V. R. Deline, P. Williams, and C. A. Evans, Jr., *Appl. Phys. Lett.* **32**, 276 (1978).

³S. S. Lau, M. van Allen, I. Golecki, M. A. Nicolet, E. F. Kennedy, and W. F. Tseng, *Appl. Phys. Lett.* **35**, 327 (1979).

⁴J. T. Lue, *Appl. Phys. Lett.* **36**, 73 (1980).

⁵L. Corraera and L. Pedulli, *Appl. Phys. Lett.* **37**, 55 (1980).

⁶K. Nishiyama, M. Arai, and N. Watanabe, *Jpn. J. Appl. Phys.* **19**, L563 (1980).

⁷A. Gat, *Electron Dev. Lett.* **EDL-2**, 5 (1981).

⁸R. A. Powell, T. O. Yep, and R. T. Fulks, *Appl. Phys. Lett.* **39**, 150 (1981).